Physicochemical Properties of VPI-5

Mark E. Davis,*,† Consuelo Montes,† Paul E. Hathaway,† Juan P. Arhancet,† Dennis L. Hasha,‡ and Juan M. Garces§

Contribution from the Department of Chemical Engineering, Virginia Polytechnic Institute and State University, Blacksburg, Virginia 24061, and Dow Chemical Company, Midland, Michigan 48640. *Received September 26, 1988*

Abstract: Infrared, solid-state NMR, and physical adsorption data of aluminophosphate molecular sieve VPI-5 are consistent with those expected from the crystal structure. Rhodium-impregnated VPI-5 hydrogenates larger olefins than other rhodium-containing molecular sieves.

Virginia Polytechnic Institute Number 5 is a family of aluminophosphate-based molecular sieves, which share a common three-dimensional topology containing rings of 18 T-atoms.[1] The extra-large pores of VPI-5 are unidimensional channels circumscribed by rings consisting of 18 T-atoms and possess free diameters of approximately 12 Å. Preliminary adsorption data[1] confirm the existence of the extra-large pores.

We report the detailed physicochemical properties of VPI-5 and compare them with those of $AlPO_4$-5[2] and $AlPO_4$-11.[2]

Experimental Section

a. Samples. The molecular sieves $AlPO_4$-11 and $AlPO_4$-5 were synthesized according to the procedures outlined in examples 32 and 3, respectively, in the Union Carbide Patent.[3] VPI-5 can be synthesized with a variety of organic agents such as amines and quaternary ammonium cations. All data reported here for VPI-5 are from samples prepared with tetrabutylammonium hydroxide[4] since these materials show greater thermal and hydrothermal stability than those synthesized with di-*n*-propylamine.

b. Analysis. The magic angle spinning ^{27}Al spectrum was recorded on a Bruker CXP 200 spectrometer. The ^{27}Al spectrum was obtained at a frequency of 52.15 MHz and a rotation rate of 3–5 kHz. The ^{27}Al chemical shifts are reported relative to $Al(NO_3)_3$ in aqueous solution at infinite dilution and are not corrected for second-order quadrupole effects. The ^{31}P spectra were taken at 81.0 MHz with a spinning rate of 4.5–5 kHz on a Bruker MSL 300 spectrometer at the Bruker Applications Laboratory in Billerica, MA. Chemical shifts are reported relative to 85 wt % H_3PO_4.

Thermogravimetric analyses (TGA) and differential scanning calorimetry (DSC) were performed in air on a Du Pont 951 thermogravimetric analyzer and a Perkin-Elmer DSC-4, respectively.

Diffuse reflectance, infrared measurements were performed on neat samples using an IBM IR/32 FTIR equipped with a Spectra-Tech Inc. diffuse reflectance cell, which is coupled to a gas-handling system. Transmission, infrared measurements were performed on a Nicolet 5DXB FTIR using samples that were mixed with KBr and pressed into disks.

Adsorption capacities of vapor-phase adsorbates and complete oxygen and water isotherms were measured using a McBain–Bakr balance. Complete argon adsorption isotherms and helium pycnometry were performed using an Omnisorp 100 analyzer.

Results and Discussion

Structures. Figure 1 illustrates the [100] projection of $AlPO_4$-11[5,6] and the [001] projections of $AlPO_4$-5[7,8] and VPI-5.[9] In each molecular sieve, the largest pore is unidimensional and lined exclusively with 6-membered rings.

Table I gives the free diameter of the largest pore and the framework density of $AlPO_4$-11, $AlPO_4$-5, and VPI-5. $AlPO_4$-11 contains an elliptical pore while $AlPO_4$-5 and VPI-5 possess circular ones. The framework density (FD) is defined as the number of T-atoms per 1000 Å^3.[6] For zeolite frameworks, the FD's observed range from 12.5 to around 20.5.[6] The FD is related to the pore volume; the lower the FD, the larger the pore volume.

Table I lists also the total void volume and the void volume of the unidimensional pore system in each of the molecular sieves. These data are calculated from the crystal structure assuming an aluminophosphate framework density of 2.60 ± 0.05 g/cm^3. Water[1] and helium pycnometry results are consistent with this framework density. The total and unidimensional void volumes are predicted for comparison with experimentally measured volumes (vide infra) obtained from water and oxygen adsorption isotherms, respectively.

Composition. The bulk chemical composition of a typical as-synthesized sample of VPI-5 prepared with tetrabutylammonium hydroxide is 0.18 wt % C, <0.1 wt % N, 16.85 wt % Al, and 18.32 wt % P. The atomic Al/P ratio is 1 within experimental error. However, notice the low carbon and nitrogen contents. For comparison, $AlPO_4$-5 and $AlPO_4$-11 synthesized with tetrapropylammonium and di-*n*-propylamine, respectively, give 7.5 wt % C, 0.67 wt % N, and 5.1 wt % C, 1.0 wt % N, respectively.[3] The organic present in $AlPO_4$-5 and $AlPO_4$-11 has been shown to correspond to tetrapropylammonium and di-*n*-propylamine, filling the volume of the 12 and 10 T-atom pores, respectively.[10] Since the carbon and nitrogen contents of VPI-5 are so low the structure of the residual organic cannot be determined. Attempts to obtain ^{13}C NMR results were unsuccessful.

Figure 2 shows the TGA and DSC results for VPI-5. The endotherm and weight loss illustrated are caused by the removal of water up to ~24 wt % (verified by on-line mass spectrometry). No further weight losses were observed when heating to above 800 °C. The TGA results are influenced by the heating rate. At heating rates slower than 2 °C/min, the water loss is occurring in different stages. Thus, water is residing in several environments within VPI-5. The TGA/DSC results that are unique to VPI-5 are distinguishable from those of other $AlPO_4$ molecular sieves by (i) the large weight loss due to the desorption of water and (ii) the absence of a strong exothermic peak and associated weight loss from the combustion of the organic, which is typically at an amount equivalent to pore filling. Examples of TGA/DTA patterns for other aluminophosphate and silicoaluminophosphate molecular sieves can be found elsewhere.[11,12]

The elemental and thermal analyses indicate that the organic structure-directing agent (tetrabutylammonium) used to crystallize

† Virginia Polytechnic Institute and State University.
‡ The Analytical Laboratories, Dow Chemical Co.
§ The Inorganic Materials and Catalysis Laboratories, Dow Chemical Co.

(1) Davis, M. E.; Saldarriaga, C.; Montes, C.; Garces, J.; Crowder, C. *Zeolites* **1988**, *8*(5), 362–367.
(2) Wilson, S. T.; Lok, B. M.; Messina, C. A.; Cannan, T. R.; Flanigen, E. M. *J. Am. Chem. Soc.* **1982**, *104*, 1146–1147.
(3) Wilson, S. T.; Lok, B. M.; Flanigen, E. M. U.S. Patent 4310440, 1982.
(4) Davis, M. E.; Montes, C.; Garces, J. *ACS Symp. Ser.*, in press.
(5) Bennett, J. M.; Richardson, J. W.; Pluth, J. J.; Smith, J. V. *Zeolites* **1987**, *7*, 160–162.
(6) Meier, W. M.; Olson, D. H. *Atlas of Zeolite Structure Types*, 2nd ed.; Butterworths: London, 1987.
(7) Bennett, J. M.; Cohen, J. P.; Flanigen, E. M.; Pluth, J. J.; Smith, J. V. *ACS Symp. Ser.* **1983**, *218*, 109–118.
(8) Richardson, J. W.; Pluth, J. J.; Smith, J. V. *Acta Crystallogr.* **1987**, *C43*, 1469–1472.
(9) Crowder, C.; Garces, J. M.; Davis, M. E. *Adv. X-Ray Anal.*, in press.
(10) Flanigen, E. M.; Patton, R. L.; Wilson, S. T. *Stud. Surf. Sci. Catal.* **1988**, *37*, 13–27.
(11) Sierra de Saldarriaga, L.; Saldarriaga, C.; Davis, M. E. *J. Am. Chem. Soc.* **1987**, *109*, 2686–2691.
(12) Hasha, D.; Sierra de Saldarriaga, L.; Saldarriaga, C.; Hathaway, P. E.; Cox, D. F.; Davis, M. E. *J. Am. Chem. Soc.* **1988**, *110*, 2127–2135.

0002-7863/89/1511-3919$01.50/0

Table I. Properties Derived from Crystal Structures

molecular sieve	framework density (FD), TO_2, 1000 Å^3	ring sizes	free diameter of pore,[a] Å	total void volume,[b] cm^3/g	unidimension at pore void volume,[b] cm^3/g
$AlPO_4$-11	19.1	4, 6, 10	6.3 × 3.9 elliptical	0.134	0.080
$AlPO_4$-5	17.5	4, 6, 12	7.3 circular	0.180	0.147
VPI-5	14.2	4, 6, 18	12.1 circular	0.310	0.255

[a] Based upon an oxygen radius 1.30–1.35 Å. [b] Assumes a density of 2.6 ± 0.05 g/cm^3 for the aluminophosphate framework.

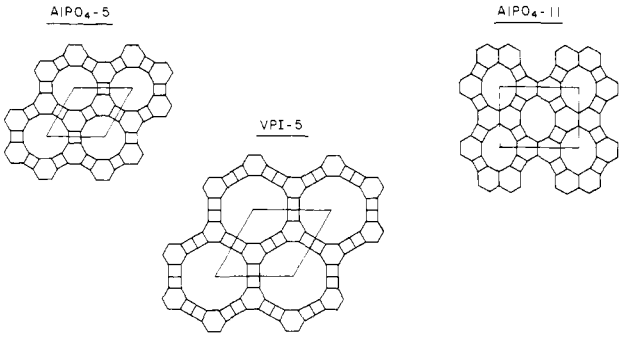

Figure 1. Framework [100] projection of $AlPO_4$-11 and framework [001] projections of $AlPO_4$-5 and VPI-5.

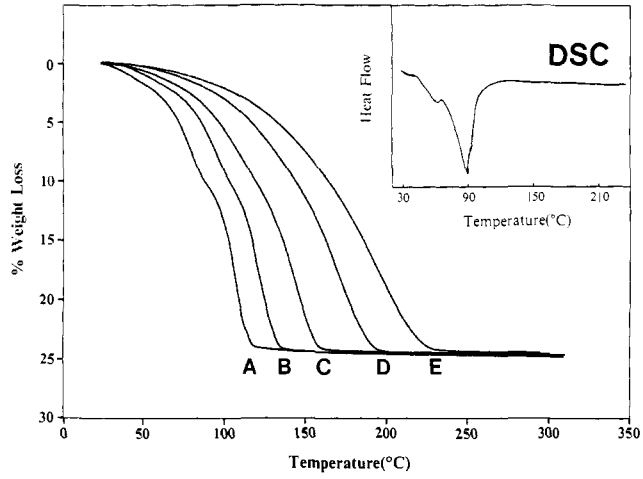

Figure 2. Thermogravimetric analyses of VPI-5. Heating rate: (A) 1 °C/min, (B) 2 °C/min, (C) 8 °C/min, (D) 15 °C/min, (E) 30 °C/min. (Inset) Differential scanning calorimetry of VPI-5. Heating rate = 1 °C/min.

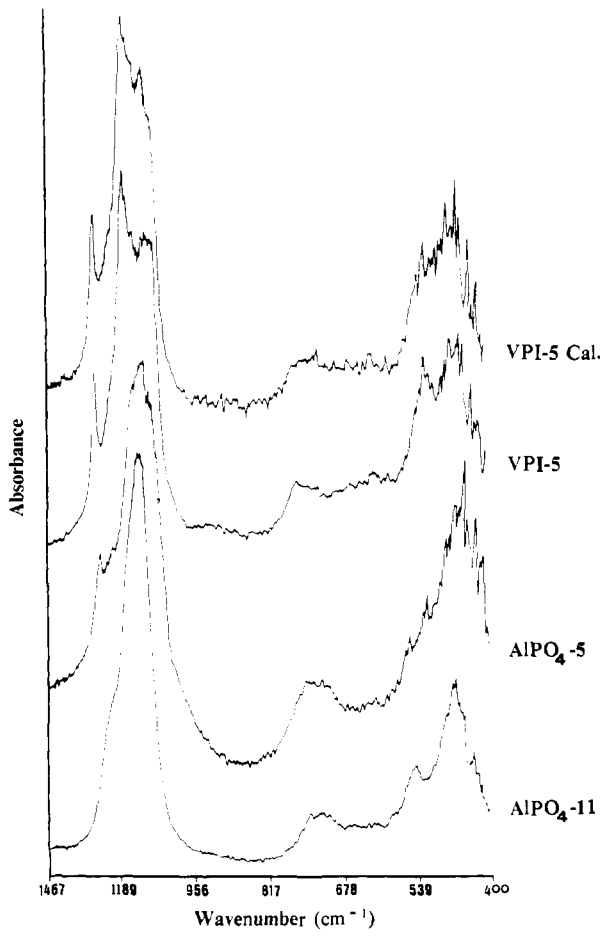

Figure 3. Infrared spectra of the structural region for molecular sieves.

VPI-5 does not reside within the extra-large pores in a space-filling capacity in contrast with other aluminophosphate molecular sieves. We have interpreted these results along with other findings concerning crystallization behavior as indications of a new type of crystallization mechanism. Studies involving the crystallization mechanism of VPI-5 are in progress, and preliminary results will be reported elsewhere.[13]

Infrared Analysis. Figure 3 shows infrared spectra for KBr disks of $AlPO_4$-11, $AlPO_4$-5, and VPI-5. The $AlPO_4$-5 spectrum agrees with that of van Nordstrand et al.[14] Peaks around 1200–1000, 740–715, and 475–460 cm^{-1} are common to $AlPO_4$-11, $AlPO_4$-5, and VPI-5 as expected since all three sieves contain 4- and 6-membered rings. $AlPO_4$-5 and VPI-5 give a band at around 1265 cm^{-1} while $AlPO_4$-11 shows only a shoulder at 1220 cm^{-1}. Although we suspect that the strong absorbance in the region of 1200–1000 cm^{-1} is from several overlapping bands in all three molecular sieves, it is most evident in VPI-5. A sample of VPI-5 was heated under vacuum from room temperature to 550 °C at 2 °C/min and then exposed to humid air (bubbled through water). The room-temperature infrared spectrum (labeled VPI-5 Cal) is nearly identical with that from the as-synthesized material. This result along with X-ray powder diffraction, solid-state NMR (vide infra), and adsorption (vide infra) data suggests that the VPI-5 structure remains essentially intact after the high-temperature treatment outlined above.

Infrared spectra of the hydroxyl region were obtained on neat samples using diffuse reflectance. A single, weak hydroxyl band is observed from each aluminophosphate. For $AlPO_4$-11 and $AlPO_4$-5, the hydroxyl band is at 3676 and 3677 cm^{-1}, respectively. These results compare well with those of Flanigen et al.[10] who reported hydroxyl bands for $AlPO_4$-11 and AlPO4-5 at 3675 and 3679 cm^{-1}, respectively. These bands are most likely due to P–OH groups on the surface of the crystals and at internal defect sites. For VPI-5, a single weak band is observed also and is at a frequency of 3675 cm^{-1}.

^{27}Al and ^{31}P NMR Results. Figure 4 shows the ^{27}Al and ^{31}P NMR spectra of as-synthesized VPI-5. The ^{27}Al spectrum gives a sharp resonance at 36.3 ppm, a diffuse peak at 28 ppm, and a broad band at −15 to −45 ppm. The peak at 36.3 ppm is indicative of aluminum, which is tetrahedrally coordinated and linked to four phosphorus neighbors via bridging oxygen atoms.[11,12,15,16] The intensity around 28 ppm and that from −15 to −45 ppm could indicate that certain framework sites are in-

(13) Davis, M. E.; Montes, C.; Hathaway, P. E.; Garces, J. Eighth International Zeolite Conference, in press.
(14) van Nordstrand, R. A.; Santilli, D. S.; Zones, S. I. *ACS Symp. Ser.* **1988**, *368*, 236–245.
(15) Blackwell, C. S.; Patton, R. L. *J. Phys. Chem.* **1984**, *88*, 6135–6139.
(16) Blackwell, C. S.; Patton, R. L. *J. Phys. Chem.* **1988**, 92, 3965–3970.

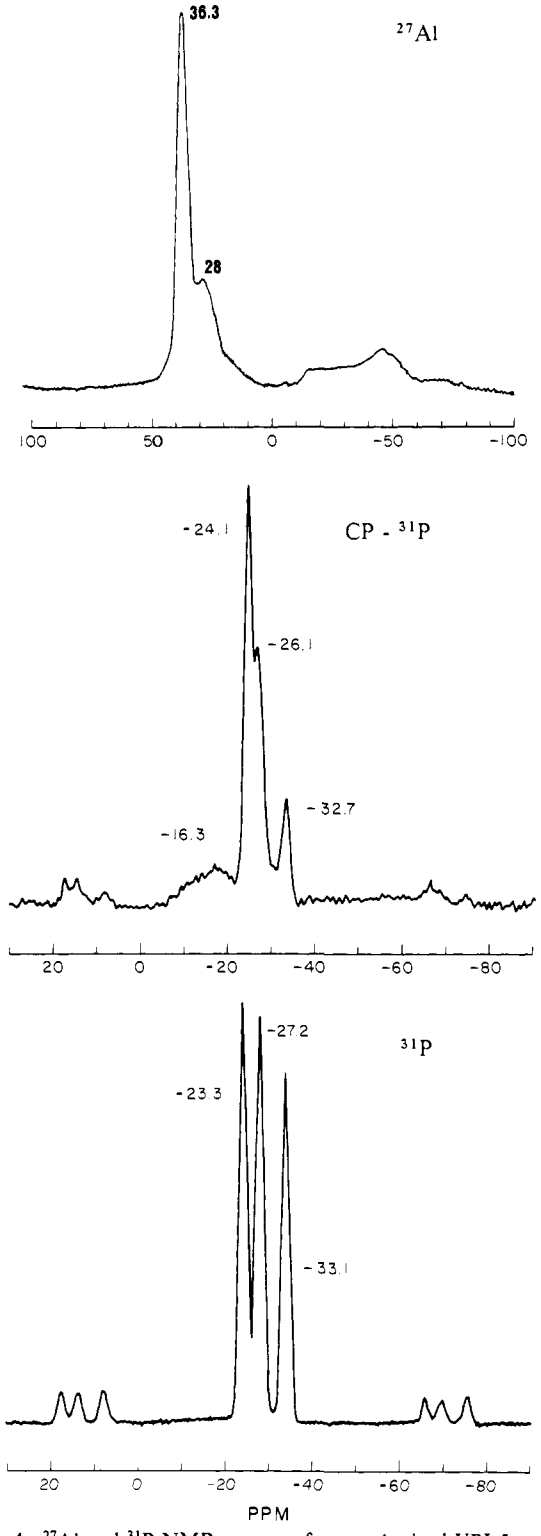

Figure 4. ^{27}Al and ^{31}P NMR spectra of as-synthesized VPI-5.

teracting with water to increase their coordination. The effect of hydration of ^{27}Al NMR spectra has appeared.[11,12,15,16] By varying the spinning rate, we have ascertained that a portion of the intensity in the region of −15 to −45 ppm is a spinning side band. Features similar to those in the 28 and −15 to −45 ppm range of VPI-5 have been observed with other aluminophosphates.[15] The VPI-5 sample heated to 550 °C as previously described and rehydrated shows a main resonance at 40.2 ppm with a small shoulder at 30.4 ppm. The loss of intensity in the −15 to −45 ppm range and the shift in the position of the main resonances suggest the environments of aluminum have been slightly altered by the 550 °C treatment.

The ^{31}P spectrum of VPI-5 is quite unusual. The VPI-5 structure contains two crystallographically unique phosphorus sites. These sites are located in the 6-membered rings (S1) (see [001] projection in Figure 1) and in the atomic positions that belong to the two adjacent 4-membered rings (S2) and are in an atomic ratio of 2/1, respectively. Also, it has been shown recently that crystallographically unique phosphorus sites can give distinct ^{31}P NMR peaks.[16] Here, we show that the number of ^{31}P NMR resonances exceeds the number of unique crystallographic phosphorus sites. However, occluded template molecules have been reported to influence the ^{31}P NMR spectrum of silicoaluminophosphates.[12] The resonances caused by the organic are removed by calcining the sieves in air at 550 °C.[12] The VPI-5 sample heated at 550 °C as previously described and rehydrated shows a ^{31}P NMR spectrum similar to that illustrated in Figure 4. Thus, none of the resonances are due to the influence of the residual organic. A sample of VPI-5 evacuated at room temperature gives ^{31}P NMR resonances at −27 and −32 ppm in an area ratio that closely approximates 2/1. The peak at −23 ppm is no longer present. From these results we conclude that the resonance at −27 ppm is from phosphorus in the S1 sites and the peak at −33 ppm is from phosphorus in the S2 sites (vide supra). Since the hydrated ^{31}P NMR spectrum reveals three resonances at an approximate 1/1/1 ratio (T_1 of each peak around 30 s), it appears as if the occluded water affects half of the S1 sites only.

Cross-polarization, magic angle spinning ^{31}P NMR data on VPI-5 were obtained in order to assist in interpreting the effect of water on the ^{31}P NMR spectrum. Figure 4 illustrates the results. The resonance at −24 ppm is enhanced over the two peaks at −26 and −33 ppm, which have approximately the same area (−26 ppm peak is a shoulder of the −24 ppm peak). The greatest enhancement occurs at contact times near 1 ms. These results indicate that the water that enhances the ^{31}P NMR resonance is relatively immobile. We suspect that water in the 18 T-atom rings would be quite mobile. Thus, the variable contact time data are consistent with the enhancement due to water held relatively tightly in the 6-membered rings. The existence of different water environments is confirmed also by the TGA/DSC results (vide supra).

This is the first report of the influence of water on a ^{31}P NMR spectrum of an aluminophosphate molecular sieve. The mechanism of the water–phosphorus interaction is not clear to us at this time.

We speculate that the broad peak around −16.3 ppm in the CP ^{31}P NMR spectrum is from P–OH present in VPI-5. The concentration of these sites is small (potentiometric titration of VPI-5 with HCl and NaOH reveals little to no exchange sites), and it is probable that CP is required in order to observe their presence. If this assignment is correct, then there must be a number of different environments, e.g., on the surface and internal defects.

Adsorption Results. Table I shows the predicted values of the total and unidimensional pore void volumes calculated from the crystal structure data of $AlPO_4$-11, $AlPO_4$-5, and VPI-5. These properties can be experimentally measured by determining the micropore filling of the molecular sieves with water (total) and oxygen (unidimensional pore system only). Water has a kinetic diameter of 2.65 Å and can enter all the voids of $AlPO_4$-11, $AlPO_4$-5, and VPI-5. However, since the kinetic diameter of oxygen is 3.45 Å, it cannot diffuse through a 6-membered ring and is confined to the unidimensional pore systems of the sieves.

Figure 5 gives the water adsorption isotherm for several molecular sieves. The data for NaX, $AlPO_4$-5 (solid line), and $AlPO_4$-11 are from Union Carbide[17] while the isotherm illustrated by the dashed curve for $AlPO_4$-5 is that of Thamm et al.[18] Since the shape of the VPI-5 isotherm was unusual, the data given in the VPI-5 isotherm were obtained in two ways: (i) a single sample was used to generate the complete isotherm, and (ii) each datum

(17) Wilson, S. T.; Lok, B. M.; Messina, C. A.; Cannan, T. R.; Flanigen, E. M. *ACS Symp. Ser.* **1983**, *No. 218*, 79–106.
(18) Thamm, H.; Stack, H.; Jahn, E.; Fahlke, B. *Adsorpt. Sci. Technol.* **1986**, *3*, 217–220.

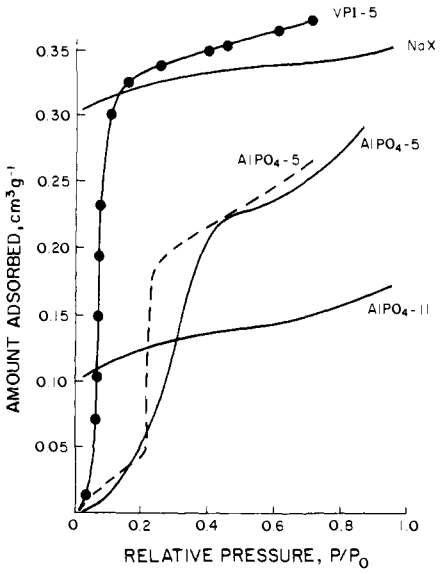

Figure 5. Water adsorption isotherms for molecular sieves at room temperature.

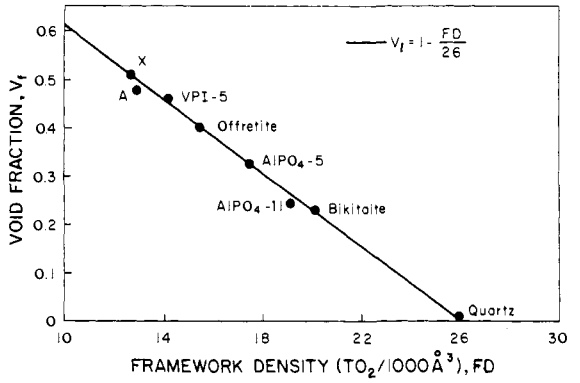

Figure 6. Relation between void fraction measured from water pore volume and the framework density.

point obtained was from a fresh sample. NaX and $AlPO_4$-11 show type I isotherms. The microporous capacity of $AlPO_4$-11 is approximately 0.13 cm^3/g, which is good agreement with the predicted value given in Table I. Thamm et al.[18] speculated that the sudden rise in the water adsorption of $AlPO_4$-5 at $P/P_0 \simeq 0.2$ may be due to coordinately bonded water. Whatever the mechanism, the same appears to occur in VPI-5. For $AlPO_4$-5, the two isotherms shown do not compare well. We will use the water isotherm reported by Thamm et al. as the correct one for $AlPO_4$-5. The microporous capacity of $AlPO_4$-5 and VPI-5 is determined at the intercept of the micropore and mesopore regions of the isotherm. Thus, the water adsorption capacity of $AlPO_4$-5 and VPI-5 is approximately 0.18 and 0.32 cm^3/g, respectively, and is in excellent agreement with the predicted values listed in Table I.

Figure 6 illustrates the relationship between the void fraction measured by the microporous water volume and the framework density. The data shown for quartz and the zeolites are from Breck[19] as is the correlation given by the solid line. The aluminophosphate results are those generated from the data shown in Figure 5. The aluminophosphate results fit quite well with Breck's correlation for zeolites.

Figure 7 shows the oxygen adsorption isotherms for several molecular sieves. The data provided for $AlPO_4$-11, $AlPO_4$-5, and NaX are from Union Carbide[17] and are for adsorption at liquid-oxygen temperature. The VPI-5 results are given at liquid-nitrogen (squares) and liquid-argon (circles) temperatures. Since all the isotherms in Figure 7 show type I behavior, the microporous

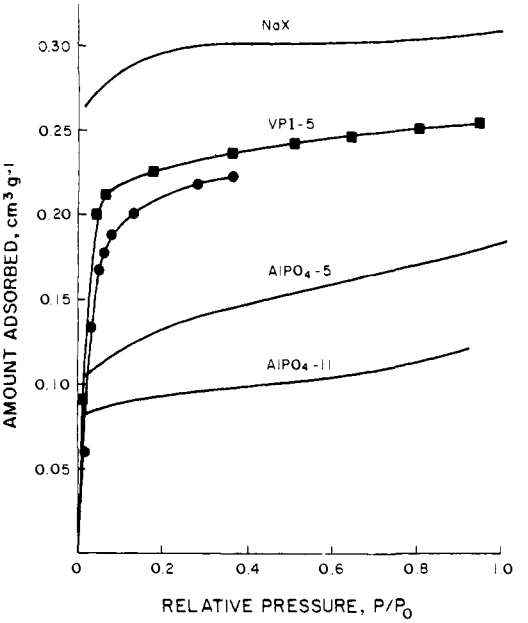

Figure 7. Oxygen adsorption isotherms for molecular sieves at liquid-oxygen temperatures. VPI-5 data at liquid-nitrogen (squares) and liquid-argon (circles) temperatures.

Table II. Adsorption Capacity of Molecular Sieves at $P/P_0 = 0.4$

kinetic diameter, Å	adsorbate[b]	capacity, cm^3/g		
		$AlPO_4$-11[a]	$AlPO_4$-5[a]	VPI-5
2.65	H_2O	0.123	0.220	0.351
3.46	O_2	0.085	0.146	0.228
4.30	*n*-hexane		0.139	0.198
6.0	cyclohexane	0.070	0.145	0.156
6.20	neopentane	0.028	0.137	0.148
8.50	triisopropylbenzene		0.021[c]	0.117

[a] Data from Union Carbide.[19] [b] Adsorption at room temperature except for O_2, which was performed at either liquid N_2 or O_2 temperatures. [c] This work.

capacity is relatively easy to ascertain (taken here at $P/P_0 = 0.4$) and is 0.085, 0.146, and 0.228 for $AlPO_4$-11, $AlPO_4$-5, and VPI-5, respectively. These data are within experimental error of the predicted values listed in Table I.

The water and oxygen adsorption isotherms of $AlPO_4$-11, $AlPO_4$-5, and VPI-5 give microporous adsorption capacities that are in excellent agreement with the values predicted from their crystal structures. Therefore, these samples are highly crystalline and do not contain detectable amounts of extraneous material, e.g. amorphous impurities, that can affect the adsorption capacities.

Table II lists the adsorption capacity of $AlPO_4$-11, $AlPO_4$-5, and VPI-5 for various adsorbates with kinetic diameters ranging from 2.65 to 8.50 Å. All values listed are obtained at $P/P_0 = 0.4$. The data for $AlPO_4$-11 and $AlPO_4$-5 (except for triisopropylbenzene) are from Union Carbide.[20] The VPI-5 data were obtained using a McBain–Bakr apparatus, and the samples were activated by heating to 350 °C under vacuum overnight. Since $AlPO_4$-11, $AlPO_4$-5, and VPI-5 all contain unidimensional channels, all adsorbates other than water should give similar capacities for a given structure. Water, of course, can penetrate the 6-membered rings and thus will show a greater capacity than all other adsorbates. The water capacities listed in Table II are not the values for microporous filling for $AlPO_4$-5 and VPI-5 as shown above but in fact include interparticle adsorption. The water capacity reported previously for VPI-5[1] was obtained at high P/P_0 and therefore contains interparticle adsorption. The actual microporous capacity is given here from the data provided in the water adsorption isotherm.

(19) Breck, D. W. *Zeolite Molecular Sieves*; Wiley: New York, 1974.

(20) Wilson, S. T.; Lok, B. M.; Messina, C. A.; Flanigen, E. M. *Proceedings of the Sixth International Zeolite Conference*; Olsen, D., Bisio, A., Eds.; Butterworths: Surrey, U.K., 1985; 97–109.

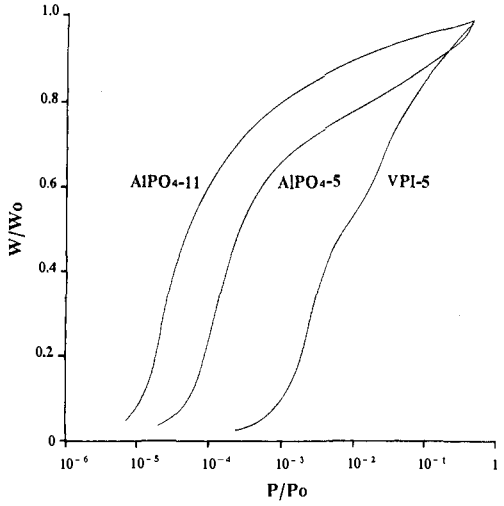

Figure 8. Argon adsorption isotherms at liquid-argon temperatures.

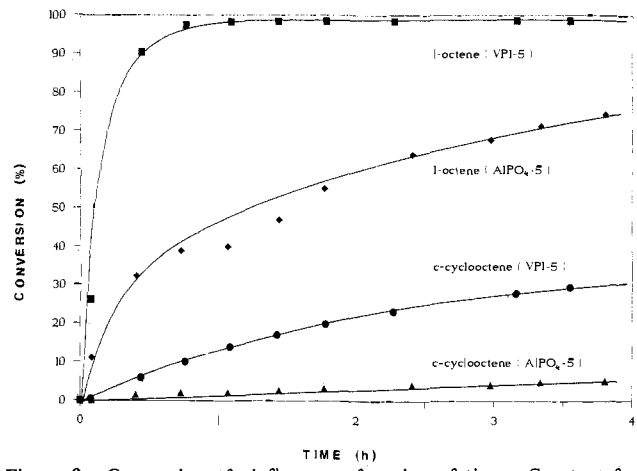

Figure 9. Conversion of olefins as a function of time. See text for experimental conditions. Conversions calculated from olefin depletions measured by gas chromatography.

$AlPO_4$-11 shows a similar adsorption capacity for oxygen and cyclohexane. These molecules are smaller than the 10 T-atom pore of $AlPO_4$-11 and can therefore be adsorbed. Neopentane is larger than the $AlPO_4$-11 pore size and is not adsorbed in any appreciable capacity. Thus, the molecular sieving effect is illustrated.

$AlPO_4$-5 adsorbs oxygen and the listed hydrocarbons except for triisopropylbenzene. The triisopropylbenzene is too large to penetrate the 12 T-atom ring. The adsorption capacity of $AlPO_4$-5 is the same, within experimental error, for all adsorbates other than water.

VPI-5 reveals two phenomena not observed in the other aluminophosphates. First, triisopropylbenzene is adsorbed. Thus, the extra-large pore is able to accommodate larger adsorbates than other molecular sieves. Second, the adsorption capacity monotonically decreases with increasing adsorbate size. Since VPI-5 contains pores that are slightly larger than 12 Å, all adsorbates other than triisopropylbenzene have the possibility of fitting more than one molecule across the diameter of the pore. In other words, packing of adsorbate molecules may be important in these extra-large pores. Further evidence to support this idea is given below.

Previously, we performed pycnometry experiments on VPI-5 with both liquid triisopropylbenzene and water in order to determine microporous adsorption of triisopropylbenzene.[1] Densities of 2.56 and 1.64 g/cm^3 were measured with water and triisopropylbenzene, respectively. At that time, we assumed the total, microporous, void volume was 0.384 cm^3/g as obtained from water vapor adsorption. As described previously in this report, the actual total, microporous void volume is approximately 0.32 cm^3/g. If we repeat our previous calculations[1] using the correct total microporous void volume, the pore volume of VPI-5 as measured by triisopropylbenzene adsorption from the liquid phase is 0.10 cm^3/g. Notice that this capacity is within the experimental error of the uptake measured in the vapor-phase experiment at P/P_0 = 0.4 (see Table II). Thus, triisopropylbenzene does adsorb into the microporous voids of VPI-5.

Complete argon adsorption isotherms for $AlPO_4$-11, $AlPO_4$-5, and VPI-5 were measured at liquid-argon temperatures and are illustrated in Figure 8. The same isotherm as shown in Figure 8 is obtained from the VPI-5 sample that was treated at 550 °C as described above. If the shape of the isotherm is primarily a function of pore diameter, then the initial transition region of the isotherm should occur at P/P_0 proportional to the size of the pore; i.e., the larger the pore, the larger the P/P_0 at which the transition occurs. This has been shown to be true for zeolites when argon is used as the adsorbate.[21] Here we display the same trend with $AlPO_4$-11, $AlPO_4$-5, and VPI-5. Notice the difference in the transition P/P_0 for the 10, 12, and 18 T-atom rings. The second transition at $5 \times 10^{-2} < P/P_0 < 10^{-2}$ for VPI-5 is not observed with $AlPO_4$-11 and $AlPO_4$-5. A second transition is reported also for ZSM-5.[21-24] The nature of this phenomenon has been the subject of speculation[22-24] and involves adsorbate–adsorbate interactions. Thus, if molecular packing occurs in VPI-5 with argon, then adsorbate–adsorbate interactions may be influencing the adsorption isotherm. We are currently studying this issue further by collecting adsorption isotherms with neopentane[25] since it may be too large to fit more than a single molecule across the diameter of the unidimensional pores of VPI-5. The neopentane adsorption isotherm at 0 °C does not reveal a second transition.

Catalytic Hydrogenation of Olefins. $AlPO_4$-5 and VPI-5 were impregnated with rhodium by the following procedure. The complex $Rh(CO)_2(acac)$ was dissolved in acetone. The sieves were slurried in the rhodium solution overnight after which the acetone was removed by evacuation. Rh–$AlPO_4$-5 and Rh–VPI-5 each contained approximately 1 wt % Rh. Exposure to hydrogen at 30 °C (1 atm) caused these materials to become black (a good indication of rhodium metal). Approximately 0.1 g of each solid was vigorously agitated in 20 cm^3 of a reactant solution, which was 2 wt % 1-octene and 2 wt % *cis*-cyclooctene in a decane solvent, and the mixture blanketed with hydrogen fixed at 1 atm pressure. Since we expected that some of the rhodium would be on the exterior of the $AlPO_4$-5 and VPI-5 crystals, a 50 mol excess (compared to rhodium) of tri-*o*-tolylphosphine was added also. The bulky phosphine should poison surface rhodium.[26] We confirmed the poisoning of surface rhodium by contacting Rh–$AlPO_4$-5 with dimethylcyclooctene in decane at 30 °C (1 atm) of hydrogen with a 50 mol excess of tri-*o*-tolylphosphine added and observing that no reaction products were produced over a period of 12 h.

The results of hydrogenating 1-octene and *cis*-cyclooctene with Rh–$AlPO_4$-5 and Rh–VPI-5 are given in Figure 9. The 1-octene and *cis*-cyclooctene are readily hydrogenated with Rh–VPI-5. The Rh–$AlPO_4$-5 converts the 1-octene but very slowly reacts the *cis*-cyclooctene. Thus, the conversion of large molecules not readily reacted in all other molecular sieves, which contain 12 T-atom ring or less, is demonstrated by the hydrogenation of *cis*-cyclooctene using Rh–VPI-5. The Rh–$AlPO_4$-5 results are comparable to those obtained from Rh–NaX by Huang and Schwartz.[26] Since $AlPO_4$-5 and NaX both contain pores consisting of 12 T-atoms, the similarity in the data from Rh–$AlPO_4$-5 and Rh–NaX appears reasonable.

The hydrogenation of 1-octene and *cis*-cyclooctene is the first

(21) Venero, A. F.; Chiou, J. N. *MRS Symp. Proc.* **1988**, *111*, 235–240.

(22) Jacobs, P. A.; Beyer, H. K.; Valyon, J. *Zeolites* **1981**, *1*(3), 161–169.
(23) Müller, U.; Unger, K. K. *Stud. Surf. Sci. Catal.* **1988**, *39*, 101–108.
(24) Müller, U.; Unger, K. K.; Pan, D.; Mersmann, A.; Grillet, Y.; Rouquerol, F.; Rougerol, J. Presented at the Symposium on Zeolites as Catalysts, Sorbents, and Detergent Builders, Würzberg, FRD, Sept 1988.
(25) Hathaway, P. E.; Davis, M. E., in preparation.
(26) Huang, T. N.; Schwartz, J. *J. Am. Chem. Soc.* **1982**, *104*, 5244–5245.

report of catalytic chemistry with a VPI-5 molecular sieve. The data show that catalysis can be performed in the extra-large pores of VPI-5. Since (i) rhodium is an extremely active hydrogenation catalyst, (ii) the temperature is low, and (iii) the reaction is occurring in the liquid phase, we expect that the results shown in Figure 9 are strongly influenced by the effects of diffusion for both Rh-VPI-5 and Rh-$AlPO_4$-5. If such is the case, then the data in Figure 9 could be illustrating the relative effective diffusivities of 1-octene and *cis*-cyclooctene in Rh-$AlPO_4$-5 and Rh-VPI-5. The data are consistent with this thought in that 1-octene is converted faster (i) with Rh-VPI-5 than Rh-$AlPO_4$-5 and (ii) than *cis*-cyclooctene in Rh-VPI-5.

Acknowledgment. Financial support was provided by the National Science Foundation and the Dow Chemical Co. under the Presidential Young Investigator Award to M.E.D. We thank Martin Zeiliox of the Bruker Applications Laboratory for CP ^{31}P NMR spectra, Steve Froelicher of the Dow Chemical Co. for performing TGA/mass spectroscopy experiments, and J. Merola of the Chemistry Department at VPI for $Rh(CO)_2(acac)$.

Use of a Recombinant Bacterial Fructose-1,6-diphosphate Aldolase in Aldol Reactions: Preparative Syntheses of 1-Deoxynojirimycin, 1-Deoxymannojirimycin, 1,4-Dideoxy-1,4-imino-D-arabinitol, and Fagomine

Claus H. von der Osten,[†] Anthony J. Sinskey,*[,†] Carlos F. Barbas, III,[‡] Richard L. Pederson,[‡] Yi-Fong Wang,[‡] and Chi-Huey Wong*[,‡]

Contribution from the Department of Biology, Massachusetts Institute of Technology, Cambridge, Massachusetts 02139, and the Department of Chemistry, Texas A&M University, College Station, Texas 77843. *Received August 1, 1988. Revised Manuscript Received January 6, 1989*

Abstract: A combined enzymatic aldol condensation and catalytic intramolecular reductive amination has been used in the high-yield asymmetric synthesis of polyhydroxylated alkaloids including 1-deoxynojirimycin, 1-deoxymannojirimycin, 1,4-dideoxy-1,4-imino-D-arabinitol, and fagomine. The *Escherichia coli* Zn^{2+}-containing fructose-1,6-diphosphate aldolase overexpressed in *E. coli* was used for the syntheses. The enzyme in aqueous solution containing 0.3 mM $ZnCl_2$ has excellent stability with a half-life of 60 days, compared to 2 days for the enzyme from rabbit muscle. The reactions were carried out under mild conditions without protection of functional groups. Either dihydroxyacetone phosphate or a mixture of dihydroxyacetone and inorganic arsenate can be used as donor in the aldol reactions. The aldol acceptors (*R*)- and (*S*)-3-azido-2-hydroxypropanal were prepared via lipase-catalyzed resolution of the racemic acetal precursor.

Recent studies have demonstrated the synthetic utility of aldolase-catalyzed reactions.[1-10] Of more than 15 aldolases found in nature, the metal-free, Schiff base forming fructose-1,6-diphosphate (FDP) aldolase from rabbit muscle is the most often used.[1-6] The enzyme is highly specific for dihydroxyacetone phosphate (**1a**), but accepts a variety of aldehydes as a second substrate. The donor **1a** can be generated from FDP in situ[1-4] or replaced with a mixture of dihydroxyacetone (**1b**) and inorganic arsenate (As).[2] The stereochemistry of the C-C bond formation is completely controlled by the enzyme and is the same with all substrates tested so far. Although the enzyme is commercially available, the requirement for its isolation from the mammalian source and the instability of this enzyme may circumvent its use in large-scale processes. The Zn^{2+}-containing FDP aldolase was found in many microorganisms such as *Escherichia coli*,[11] but the use of this enzyme in organic synthesis was not reported. We describe here our study of *E. coli* FDP aldolase[12] as a synthetic catalyst.

An interesting finding in this research is that the Zn^{2+}-aldolase seems to have the same substrate specificity as that of rabbit muscle FDP aldolase, accepting all the aldehyde substrates used before[2,3] for the rabbit enzyme. In aqueous solution, the microbial enzyme, however, showed excellent stability in the presence of 0.3 mM $ZnCl_2$. The estimated half-life of the free enzyme at room temperature is 60 days while that of the rabbit enzyme is 2 days (Figure 1).

To illustrate the use of the microbial enzyme in preparative-scale synthesis, the polyhydroxylated alkaloids 1,5-dideoxy-1,5-imino-D-glucitol (1-deoxynojirimycin, **5**), 1,5-dideoxy-1,5-imino-D-mannitol (1-deoxymannojirimycin, **6**), 1,4-dideoxy-1,4-imino-D-arabinitol (**7**), and 1,2,5-trideoxy-1,5-imino-D-arabinitol (fagomine,

[†] Massachusetts Institute of Technology.
[‡] Texas A&M University.

(1) Wong, C.-H.; Whitesides, G. M. *J. Org. Chem.* **1983**, *48*, 3199. Wong, C.-H.; Mazenod, F. P.; Whitesides, G. M. *Ibid.* **1983**, *48*, 3493.

(2) Durrwachter, J. R.; Drueckhammer, D. G.; Nozaki, K.; Sweers, H. M.; Wong, C.-H. *J. Am. Chem. Soc.* **1986**, *108*, 7812. In solution, **1b** reacts spontaneously and reversibly with arsenate to form dihydroxyacetone arsenate ester, a mimic of **1a**, which is accepted as a substrate by the enzyme. In the reverse reaction, the probability for the formation of the 6-arsenate is relatively low, accounting for the slow reverse reaction. For mechanistic study of the arsenate reaction, see: Drueckhammer, D. G.; Durrwachter, J. R.; Pederson, R. L.; Crans, D. C.; Wong, C.-H. *J. Org. Chem.* **1989**, *54*, 70.

(3) (a) Durrwachter, J. R.; Wong, C.-H. *J. Org. Chem.* **1988**, *53*, 4175. (b) Pederson, R. L.; Kim, M.-J.; Wong, C.-H. *Tetrahedron Lett.* **1988**, *29*, 4645.

(4) Bednarski, M. D.; Waldmann, H. J.; Whitesides, G. M. *Tetrahedron Lett.* **1986**, *27*, 5807.

(5) Wong, C.-H. In *Enzymes as Catalysts in Organic Synthesis*; Schneider, M. P., Ed.; D. Reidel Publishing Co.: Dordrecht, 1986; p 199.

(6) Mocali, A.; Aldinucci, D.; Paoletti, F. *Carbohydr. Res.* **1985**, *143*, 288. Kapusinski, M.; Franke, F. P.; Flanigan, I.; MacLeod, J. K.; Williams, J. F. *Ibid.* **1985**, *140*, 69.

(7) Kim, M. J.; Hennen, W. J.; Sweers, H. M.; Wong, C.-H. *J. Am. Chem. Soc.* **1988**, *110*, 6481.

(8) Auge, C.; Gautheron, C. *J. Chem. Soc., Chem. Commun.* **1987**, 859 and references cited therein. David, S.; Auge, C. *Pure Appl. Chem.* **1987**, *59*, 1501.

(9) Reimer, L. M.; Conley, D. L.; Pompliano, D. L.; Frost, J. W. *J. Am. Chem. Soc.* **1986**, *108*, 8010.

(10) Bednarski, M. D.; Crans, D. C.; DiCosimo, R.; Simon, E. S.; Stein, P. D.; Whitesides, G. M. *Tetrahedron Lett.* **1988**, *29*, 427.

(11) Richards, O. C.; Rutter, W. J. *J. Biol. Chem.* **1961**, *236*, 3177. Smith, G. M. *Fed. Proc.* **1980**, *39*, 1859. Belasco, J. G.; Knowles, J. R. *Biochemistry* **1983**, *22*, 122-9. Baldwin, S. A.; Perham, R. N.; Stribling, O. *Biochem. J.* **1978**, *169*, 633-41. Sugimoto, S.; Nosoh, Y. *Biochem. Biophys. Acta* **1971**, *235*, 210-21. Hill, H. A. O.; Lobb, R. R.; Sharp, S. L.; Stokes, A. M.; Harris, J. I.; Jack, R. S. *Biochem. J.* **1976**, *153*, 551-60.

0002-7863/89/1511-3924$01.50/0